King Saud University

Arabian Journal of Chemistry

www.ksu.edu.sa
www.sciencedirect.com

ORIGINAL ARTICLE

Selective oxidation of styrene to benzaldehyde using soft BaFe$_2$O$_4$ synthesized by citrate gel combustion method

Ravindra Y. Pawar, Satish K. Pardeshi *

Department of Chemistry, University of Pune, Ganeshkhind, Pune 411007, India

Abstract BaFe$_2$O$_4$ spinel type catalyst is synthesized by a simple and inexpensive one-step citrate gel combustion method, the only method to synthesize soft ferrite other than the Pechini method reported earlier. The precursor and oxide are well characterized by various techniques such as thermogravimetry–differential thermal analysis, Fourier transform IR, X-ray diffraction, X-ray florescence and scanning electron microscopy. The SEM images confirm coralloid morphology of BaFe$_2$O$_4$ catalyst. BaFe$_2$O$_4$ catalyst shows high activity for styrene oxidation in the presence of H$_2$O$_2$ (30%) as an oxidant in acetone as solvent. Gas chromatography and mass spectroscopy analysis revealed that, conversion of styrene takes place selectively to benzaldehyde up to 88.5 mol% as major product with 39.9% yield. The optimization and effect of various reaction conditions on styrene conversion and product distribution were also studied. Ultrasonication exposes active sites on the surface of catalyst and breaks the hydrophobic cluster to make the reagent available. Better catalytic activity of BaFe$_2$O$_4$ is due to different site preference energies of individual ions which depend on the ionic size of barium (1.35 Å) and iron (0.67 Å), the size of interstices and temperature. The catalyst can be reused with marginal loss in activity.

1. Introduction

Spinel compounds with the general formula of AB$_2$O$_4$ are one of the most frequently encountered structure types in inorganic chemistry (Sawada, 1996). Spinel is often used as catalysts for reactions at elevated temperature due to their high temperature stability and resistance to sintering (Busca et al., 1997); MgAl$_2$O$_4$ has been considered as a material for a number of applications in high radiation environments (Clinard et al., 1984) such as electrical insulators and dielectric windows in fission reactors (Nitani et al., 2003) and so on.

* Corresponding author. Tel.: +91 020 25601394x514; fax: +91 020 25691728.
  E-mail address: skpar@chem.unipune.ac.in (S.K. Pardeshi).

Alkaline earth metal (AEM) ferrites have attracted a considerable attention due to their potential application as magnetic materials in various electronic, magnetic and microwave devices (Cabuil, 2000; Horvath, 2000; Viswanathan and Murthy, 1990; Sugimoto, 1999). The wide application of these materials is mainly due to its excellent chemical stability, high mechanical durability, and resistant to corrosion (Simmons, 1989). They have also been employed as heterogeneous catalysts and electrode materials (Bronoel et al., 1980; Grenier et al., 1981). In order to get high-powered barium ferrite, different synthesis techniques have been developed, such as micro emulsion (Liu et al., 1998), hydrothermal reaction (Liu et al., 1999), glass crystallization (Rezlescu et al., 1993), and salt-melt technique (Chin et al., 1993). The ultrafine powder of barium ferrite ($BaFe_{12}O_{19}$) was synthesized by a sol–gel combustion technique using glycine gels, the results showed that the formation of single phase barium ferrite is significantly influenced by Ba/Fe and glycine/nitrate molar ratio, the phase composition and morphology of the barium ferrite are confirmed by X-ray diffraction, transmission electron microscopy (TEM) and high resolution TEM (Meng et al., 2014). All these methods have many drawbacks such as small area of deposition, requirement of sophisticated instruments, high working cost of system, and prolonged calcination time for crystallization. When sol–gel technique (Surig et al., 1993) is used, we get high-powered ferrite material. The atomic-level blending of the constituent elements in the required stoichiometric ratio is attained in the citrate precursor complex, which enables the decomposition of the precursor directly into the final binary oxide at lower temperature, without the formation of intermediate oxide phases that delay the formation of the final oxide (Sankaranarayanan et al., 1993).

The synthesis of barium ferrite ($BaFe_2O_4$) powder by a sol–gel combustion technique is the focus of the present work, since it allows the homogeneous mixing of two metal cations and it retards particle growth via the formation of surface citrate complexes, inhibiting the agglomeration of the particles. The catalytic activity of the synthesized catalyst is tested by using selective oxidation of styrene as a model reaction. Some oxidants such as $KMnO_4$, CrO_3, and HNO_3 (Sato et al., 1996, 1997) were applied traditionally to the oxidation of various substrates, which might result in much serious pollution and some potential risks in the process of operation. In terms of atom efficiency and environment friendly, after oxygen, aqueous hydrogen peroxide (30% H_2O_2) is a very attractive oxidant for industrial applications since water is the only by-product, and it is easy to be dealt with after reactions. Selective oxidation of styrene is successfully carried out over spinel type $CaFe_2O_4$ (Pardeshi and Pawar, 2010) and $SrFe_2O_4$ (Pardeshi and Pawar, 2011) by using 30% H_2O_2 as oxidizing agent.

In this paper, we attempt to show how $BaFe_2O_4$, of Ba-Fe-O system synthesized by citrate–nitrate gel combustion route, characterized by various techniques, is better for styrene (one of the most important pro-chiral alkenes) oxidation reaction in acetone as solvent using environmentally benign oxidant H_2O_2.

2. Experimental

2.1. Preparation of catalyst

The starting materials were of A.R. grade $Fe(NO_3)_3 \cdot 9H_2O$ (99.9%), $Ba(NO_3)_2$ ($\geqslant$99%) $C_6H_8O_7 \cdot H_2O$. The chemicals were weighed and mixed according to determined proportion. The aqueous solutions of ferric nitrate and barium nitrate were mixed and added slowly with continuous stirring in the aqueous solution of citric acid for 30 min at 40 °C temperature. Then the mixed solution was evaporated slowly at high temperature, during which the Fe^{3+} and nitrate ion provided an in situ oxidizing environment for carboxylic acids, to form homogeneous mixture of metal carboxylates. When the reaction completed, the obtained solution was heated in oven for 12 h at 120 °C. The brown fluff mass was obtained which was ground into fine powder and turned into a dried precursor. Finally, powder of the dried precursor was ignited in a crucible and followed by calcination at different temperatures for 2 h with a heating rate of 10 °C per minute to obtain barium ferrite powders.

2.2. Physico-chemical characterization

The thermal transformation associated with heat treatment was studied by a thermo gravimetric-differential thermal analysis (TG–DTA) performed on a Shimadzu TG–DTA instrument with heating rate of 10 °C min^{-1}. XRD pattern was recorded at room temperature by using a D-8 Advance Bruker AXS, diffractometer with Cu Kα radiation ($\lambda = 0.15406$ nm) operated at 40 kV and 40 mA, employing Ni-filter. Data were collected at 0.02° with counting rate of 5 s per step, in the (2θ) range from 20° to 70°. The composition of $BaFe_2O_4$ calcined at 900 °C for 2 h was determined by X-ray fluorescence on a pw1400 Philips instrument. The obtained percentage of elements is compared with the calculated values.

The FTIR spectra of calcined catalysts were recorded on a Shimadzu FTIR 8400 equipped with KBr beam splitter spectrometer at a resolution of 4 cm^{-1}, finely powdered sample was mixed with small amount of KBr and pressed under pressure. The results were obtained at ambient temperature in wavelength range from 4000 to 400 cm^{-1}. A model of SEM JEOL JSM 6360 A was used to record the scanning electron microscopy (SEM) pattern.

2.3. Catalytic activity

The selective oxidation of styrene was carried out in a three necked round bottom flask (50 ml) equipped with an X-crossed Teflon coated magnetic stirrer and a reflux condenser. 10 mmol styrene [99 + %, Aldrich], 10 ml acetone, 0.1 g catalyst, 1.0 ml of hydrogen peroxide (30% aq. Merck), and (Styrene/H_2O_2)$_{molar}$ = 1 were added successively into the flask. The flask is then immersed in an oil bath at a fixed temperature and time. The reaction was carried out for different temperatures and times. The reaction products were analyzed with a gas chromatograph (Shimadzu QP5050A instrument) equipped with a DB-5 capillary column and Quadra pole detector. Helium was used as carrier gas. The GC injection volume of 2 μL and the split ratio of 25:30 were used. 3-Nitrotoluene (99 + %, Aldrich) is used as an internal standard. The styrene conversion, product selectivity and the percentage yield of the desirable product are calculated by using the equations given elsewhere (Pardeshi and Pawar, 2010).

3. Results and discussion

3.1. Characterization

3.1.1. TG–DTA study of barium iron citrate precursors

Thermo gravimetric analysis (TGA) and differential thermal analysis (DTA) were applied to the precursor particles to determine the transition temperature for the conversion of the precursor particles to barium ferrite. Fig. 1 shows the TG/DTG/DTA for the sample prepared by the citrate gel method.

The thermo chemical behavior and chemical bonding of the as-synthesized barium ferrite powder were examined by TG–DTA, the TG curve in the range of 50–900 °C is shown in Fig. 1. The total weight loss is observed up to 59.25% (calculated 60.57%) and could be attributed to four distinct processes. The first weight loss observed in the range of 50–160 °C is 6.87% (calculated 6.34%) corresponding to partial dehydration of precursor. This dehydration step is clearly seen as a peak in DTG at 196 °C. The second weight loss is 21.42% in the range of 161–230 °C corresponding to the loss of remaining water molecules and partial decomposition of citrate ligand, it matches well with the calculated value of 23.2%. The further weight loss in TG curve is of 20.23% (calculated 21.7%) in the range of 231–361 °C, corresponding to the complete decarboxylation of the precursor into mixed oxide. This is seen in the form of well defined peak at 284 °C in DTG curve. Finally the barium ferrite is formed at 615 °C by the weight loss of 10.65% which is also in good agreement with the calculated value of 9.33% because of the evaporation of adsorbed CO_2 gas. This is also seen in the form of well defined peak at 590 °C in DTG curve, which corresponds to the decarboxylation step. After 615 °C no notable weight loss was found which indicates that $BaFe_2O_4$ was formed above 615 °C, along with the trace quantity of adsorbed carbon dioxide.

The DTA curve indicates a broad endothermic peak at 154 °C, corresponding to dehydration step. Two exothermic peaks in DTA curve at 214 °C and 291 °C are attributed to the partial dehydration and decomposition of citrate ligand (46.99% weight loss in TG curve). The whole thermal process
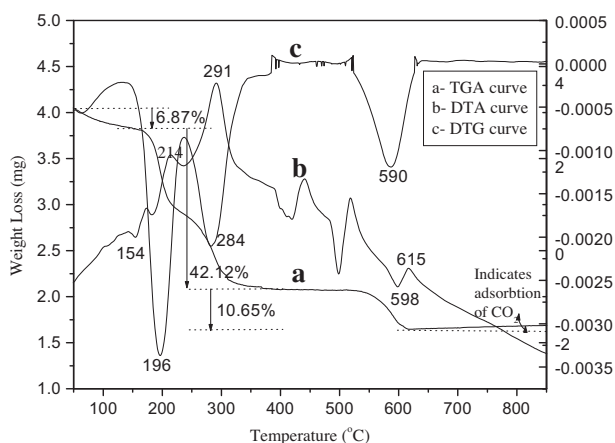
of decarboxylation is accompanied by the evolution of large amount of gas, due to vigorous oxidation reaction (Tang and Yang, 2009). Finally an endothermic peak at 598 °C in DTA indicates the transition of precursor to barium ferrite. In TG curve after 615 °C the slight mass gain is observed which indicates the adsorption of CO_2 on the surface of oxide.

3.1.2. X-ray diffraction study of barium ferrite

Fig. 2 illustrates the XRD pattern of the materials synthesized by the citrate gel method, calcined at different temperatures. The sample calcined at 900 °C, was identified as an orthorhombic spinel like phase. According to the index card the XRD pattern of precursor shows the intense peak at $2\theta = 23.9$ indicating the presence of $BaCO_3$ as shown in Fig. 2(a) with black dots. When the same precursor was calcined at 600 °C and 700 °C the new peak appeared around $2\theta = 28.4$ indicating the formation of $BaFe_2O_4$ oxide. Fe_3O_4 (peak shown with +), and $BaCO_3$ were found as intermediate phases Fig. 2 (b and c). As the calcination temperature increases to 800 °C and 900 °C there is a complete disappearance of $BaCO_3$ along with appearance of new peaks at $2\theta = 28.4, 32.7, 33.2$ and 44.16 indicating the formation of $BaFe_2O_4$ (peak shown with *) which is in good agreement with the JCPDS card No. 46-0113 from the PDF-2 database PCPDFWIN, whose lattice parameters are: $a = 19.042$ Å, $b = 5.3838$ Å and $c = 8.445$ Å at 900 °C. The calculated crystallite sizes obtained using the Scherrer formula were 40.8 nm for 800 °C (d) and 38.7 nm for 900 °C (e), respectively.

3.1.3. X-ray florescence of $BaFe_2O_4$

The elemental composition of the $BaFe_2O_4$ prepared by the citrate gel method was analyzed by the X-ray florescence method. The percentage composition of the barium and iron is in agreement with the theoretical value. The results are summarized in Table 1.

3.1.4. Scanning electron microscopy

Fig. 3 shows SEM image of barium ferrite nanoparticles as synthesized by the citrate gel method. The barium ferrite
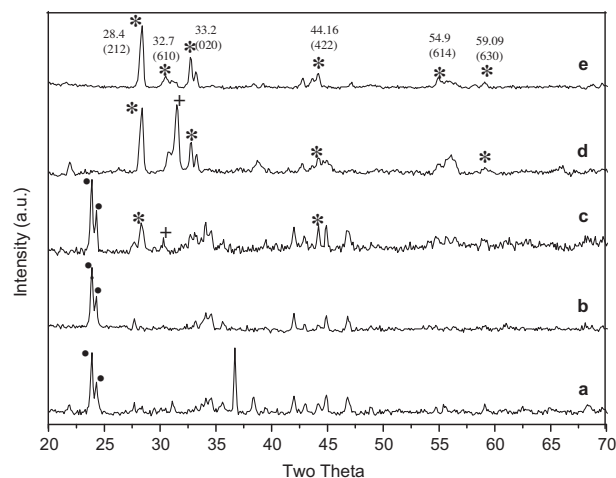

Figure 1 TG-DTG-DTA analysis of barium iron citrate precursor prepared by the citrate gel combustion method.

Figure 2 X-ray diffraction pattern of barium iron citrate precursor (a); barium ferrite powder calcined at 600 °C (b); 700 °C (c); 800 °C (d); 900 °C (e).

Table 1 Elemental analysis of $BaFe_2O_4$ catalyst by the X-ray florescence method in percentage by weight.

Barium		Iron	
Calculated	Observed	Calculated	Observed
39.1	38.4	28.8	31.2

calcined at 700 °C and 800 °C is single phase material as shown in Fig. 3(a) and (b). As shown in the SEM micrograph Fig. 3(c) and (d), barium ferrite powders annealed at 900 °C exhibit aggregates with coralloid morphology (Xu et al., 2007). When the SEM images of $CaFe_2O_4$ (Pardeshi and Pawar, 2010), $SrFe_2O_4$ (Pardeshi and Pawar, 2011) and $BaFe_2O_4$ are compared, it is seen that $BaFe_2O_4$ shows coralloid morphology with outward extending branches having an average diameter, so the total surface area of the catalyst is more than that of the other alkaline earth metal ferrites even though they are prepared by the citrate gel combustion method.

3.1.5. FTIR studies

FT-IR spectra for precursor and samples calcined at different temperatures are shown in Fig. 4. The powders calcined at different temperatures indicate that the calcination temperature can greatly influence the formation of barium ferrite. As shown in Fig. 4(a), no significant peak was found between 400 cm^{-1} and 800 cm^{-1}, which indicates that no metal oxygen bond formation takes place in precursor.

The band at 1750 cm^{-1} is assigned to the stretching vibration mode of C=O in Fig. 4(a–c). While in Fig. 4(b–e), the bands around 628–663 cm^{-1} correspond to intrinsic stretching vibration of metal ion at the tetrahedral site and the band in the range of 510–516 cm^{-1} is attributed toward the Fe—O bond vibration. Comparing the spectra (a–e) we may notice that the intensities of C=O stretching vibration at 1750 cm^{-1} and C—C stretching vibration at about 860 cm^{-1} increases up to sample (c) afterward these bands disappear completely in the spectrum (d) and (e). The disappearance of these bands indicates the formation of oxides between 800 °C and 900 °C. The bands at 1460 and 1060 cm^{-1} in Fig. 4 (a),
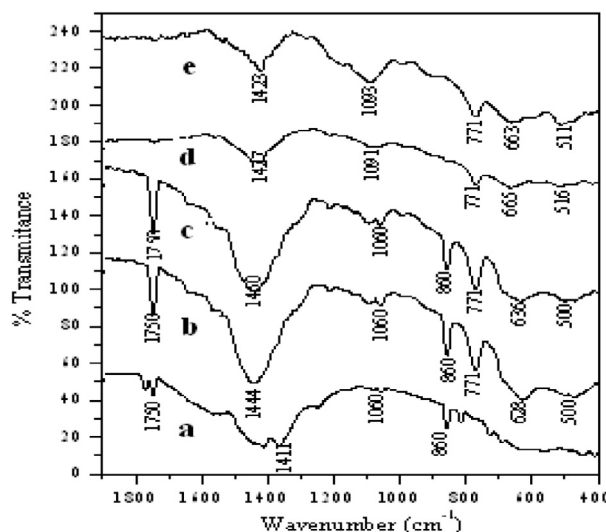
Figure 4 FTIR spectra of barium ferrite prepared by the citrate gel method calcined at different temperatures (a) precursor, (b) 600 °C, (c) 700 °C, (d) 800 °C and (e) 900 °C.

(b) and (c) indicate the presence of $BaCO_3$, while the frequency of the band decreases as the calcination temperature increases to 800 °C and 900 °C as shown in Fig. 4d and e. As the calcination temperature increases these carbonate bands were not observed due to their decarboxylation. There is a band at 2360 cm^{-1} in Fig. 4(d) and (e) which indicates the adsorption of CO_2 on the surface of catalyst, confirming the results of TG–DTA.

4. Catalytic activity studies

The oxidation of hydrocarbon to oxygenic compounds is a pivotal reaction in organic chemistry, both from the fundamental research and industrial manufacturing point of view. Now, with respect to both economic and environmental view, much attention has recently been focused on the aerobic catalytic oxidation of hydrocarbon to oxygenic compounds using metal catalysis. The metal ferrites are known to be highly efficient oxidation catalysts which have been successfully used to heterogeneously catalyze the transfer of an oxygen atom from oxidizing agent into hydrocarbon molecules in organic solvent (Smith et al., 2006).

$BaFe_2O_4$ synthesized by the citrate gel method, characterized for the structure, morphology and confirmed to be fine materials with spinel structure was then used as catalyst to evaluate its catalytic efficiency. The oxidation of styrene to benzaldehyde is used as a model reaction.

The selective oxidation of styrene proceed via radical chain mechanism in acetone as a solvent over soft $BaFe_2O_4$ catalyst as reported by Pardeshi and Pawar, 2010 to give benzaldehyde as a major product. The influence of various parameters on the styrene oxidation and the selectivity of product distribution were studied as follows.

4.1. Influence of the solvents

The influence of solvents in the catalytic oxidation of styrene was studied at 50 °C for 18 h in the presence of 30% H_2O_2
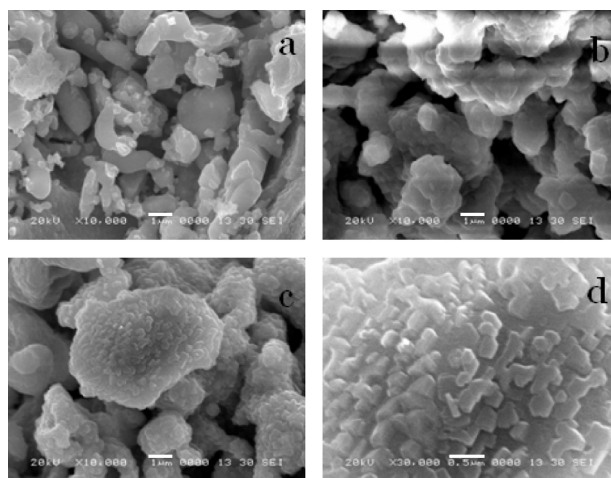

Figure 3 Scanning electron microscopy image of barium ferrite prepared by the citrate gel method calcined at (a) 700 °C, (b) 800 °C, (c) and (d) 900 °C (with different magnifications).

as oxidizing agent. The reaction when carried out in the absence of any solvent, very less styrene conversion was observed. Subsequently, the reaction was carried out using different solvents like water, methanol, ethanol, acetone and acetonitrile. The results of the effect of the solvents are shown in Fig. 5. Acetone was found to be a better solvent for this reaction. Since the solvent can influence the rate of reaction by dissolving the reactant molecules and intermediates in solution. The solvent can also affect the rate by competing with reactant molecules for active sites on the surface of heterogeneous catalyst (Ma et al., 2003). Solvent may stabilize or destabilize transition state and intermediate formed on the surface of catalyst.

However in the selective oxidation of styrene, when the reaction is carried out in polar and protic solvents like C_2H_5OH, CH_3OH and H_2O the conversion of styrene takes place up to 23.4 mol%, 28.7 mol% and 11.8 mol% with the percentage yield of benzaldehyde as 9.8, 9.4 and 6.8, respectively. When the same reaction is carried out in polar and aprotic solvent like acetone the styrene conversion increases up to 45 mol% along with 88.5 mol% of selectivity and 40% yield of benzaldehyde, respectively. On the other hand, CH_3CN is the next best polar and aprotic solvent from the viewpoint of selectivity of styrene oxide, 82.6 mol%, with respect to 15.7 mol% styrene conversion. It may be due to the fact that polar solvent like acetone with convenient liquid, dissolves a wide range of reactants and activated complex compounds are solvated without any complications. As a result the activation energy decreases and the rate of the reaction increases. Secondly in this reaction the desirable product, (benzaldehyde) is more polar than the reactant (styrene), so the reaction is accelerated in the presence of polar aprotic solvents like acetone.

4.2. Influence of reaction time

The styrene conversion and product selectivity are plotted as a function of reaction time, at 50 °C, styrene/H_2O_2 (30%) molar

ratio 1:1, in acetone as reaction medium over 0.1 g of $BaFe_2O_4$ catalyst. Under these reaction conditions, the reaction was carried out by varying the time from 6 h to 42 h. The results are shown in Fig. 6. It is found that at 6 h the conversion of styrene is only 4 mol% with 4% yield of benzaldehyde. As the reaction time increases to 12 h, styrene conversion increased to 7 mol% with 100 mol% selectivity of benzaldehyde. At 18 h styrene conversion increases up to 45.1 mol%, while the selectivity and yield of benzaldehyde are 88.6 mol% and 39.9%, respectively, along with the formation of byproducts like phenyl acetaldehyde and 1-phenyl-1, 2-ethanediol up to 9.5 mol% and 2 mol%, respectively. If the same reaction was run for 24, 30, 36 and 42 h, marginal increment is observed in styrene conversion i.e. 48.3 mol%, 50.0 mol%, 53.0 mol% and 55.0 mol%, but the selectivity of benzaldehyde suddenly decreases to 83.3 mol%, 80.0 mol%, 67.3 mol% and 66.1 mol%, respectively. The result indicates that as the reaction runs for long time the selectivity of byproducts increases up to 34 mol% at 42 h. This may be due to the complete exhaustion of H_2O_2 in the reaction mixture as the reaction runs for long duration (Kumar et al., 1995). Moreover, the impurities were also found to be formed when the reaction was allowed to run for long time. From the results it can be concluded that at 18 h the selectivity of benzaldehyde is better with respect to styrene conversion.

4.3. Influence of reaction temperature

The selective oxidation of styrene was carried out in the temperature range 30–80 °C to know the effect of temperature on the conversion of styrene and the selectivity of products (Fig. 7). The reaction when carried out at 30 °C, 14.5 mol% of styrene conversion takes place. The selectivity of benzaldehyde is 91.2 mol%, while the percentage yield of benzaldehyde is only 13.2. At 40 °C temperature the styrene conversion increases up to 26.3 mol%, while the selectivity and yield of benzaldehyde are 89.5 mol% and 23.6%, respectively. When the same reaction was carried out at 50 °C, styrene conversion steeply increases up to 45.0 mol% with 88.5 mol% selectivity
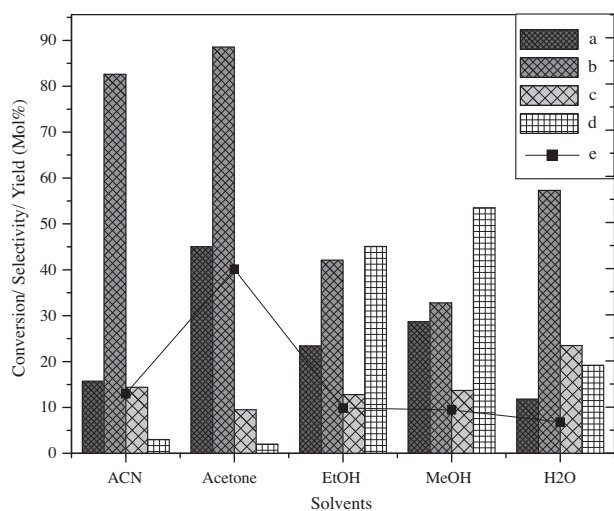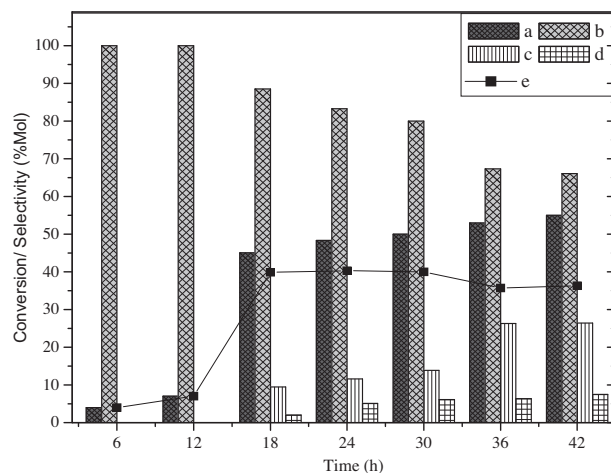

Figure 5 Effect of solvents on styrene conversion and product selectivity over $BaFe_2O_4$ catalyst, (a) styrene conversion, (b) selectivity of benzaldehyde, (c) phenyl acetaldehyde, (d) others and (e) yield of benzaldehyde.

Figure 6 Effect of reaction time on styrene conversion and product selectivity over $BaFe_2O_4$ catalyst, (a) styrene conversion, (b) selectivity of benzaldehyde, (c) phenyl acetaldehyde, (d) others and (e) yield of benzaldehyde.

of benzaldehyde. The percentage yield of benzaldehyde also increases to 40. Further increment in temperature to 60 °C, 70 °C and 80 °C results in a marginal increment in styrene conversion observed as 45.6 mol%, 48.2 mol% and 54.3 mol%, but the selectivity of benzaldehyde is prominently reduced to 81.5 mol%, 65.6 mol% and 51.4 mol%.

These results indicate that the cleavage of C=C bond is favorable with an increase in temperature up to 50 °C, but however at high temperature (80 °C) instead of C=C bond cleavage, C—O bond cleavage is done preferably, which results in an increase in byproduct like phenyl acetaldehyde and 1-phenyl-1, 2-ethanediol up to 48.6 mol%.

4.4. Influence of molar ratio of styrene/H_2O_2

The liquid phase selective oxidation of styrene was carried out with different molar ratios of styrene to H_2O_2. In all the cases, benzaldehyde is obtained as a major product along with styrene oxide and acetophenone as byproduct. It is observed that the highest conversion of styrene (45.1 mol%) as well as selectivity (88.5 mol%) and yield (39.9%) of benzaldehyde are obtained at styrene to H_2O_2 molar ratio 1:1 over BaFe$_2$O$_4$ catalyst at 50 °C for 18 h; as shown in Fig. 8. The strong interaction between catalyst and H_2O_2 inhibits the coordination of substrate and enhances desorption of the products from the active sites, which prevents the deep oxidation of benzaldehyde to benzoic acid. As the molar ratio of styrene is increased (2:1) the conversion of styrene is decreased, while the selectivity of benzaldehyde is comparatively more this may be due to less concentration of H_2O_2 which has to compete with more styrene. However, the styrene conversion is increased to 52.4 mol% for the styrene/H_2O_2 molar ratio 1:2 but the selectivity as well as the yield of benzaldehyde decrease to 44.6 mol% and 23.4%, respectively. Due to further increase in the concentration of H_2O_2 (1:3) marginal increment in the styrene conversion is observed i.e. 55.33 mol% but the selectivity and yield of benzaldehyde are distinctly decreased to
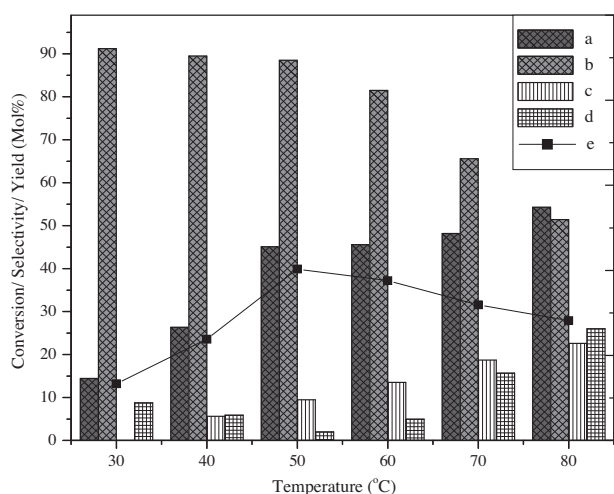

Figure 8 Effect of styrene/H_2O_2 molar ratio on styrene conversion and product selectivity over BaFe$_2$O$_4$ catalyst, (a) styrene conversion, (b) selectivity of benzaldehyde, (c) phenyl acetaldehyde, (d) others and (e) yield of benzaldehyde.
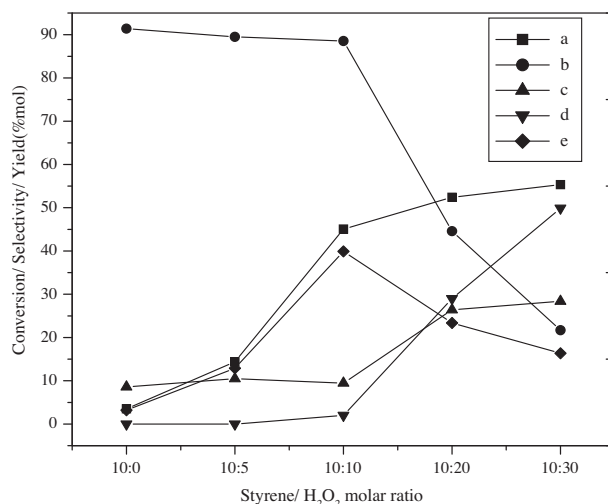
21.7 mol% and 16.35 mol%, respectively. This may be due to the excess concentration of H_2O_2 which enhances the rate of conversion of styrene, but at the same time excess water from 30% H_2O_2 hydrolyzed the intermediate i.e. styrene epoxide to form 1-phenyl-1,2-ethanediol.

4.5. The role of catalytic amount

In order to check the effect of the amount of catalyst during the selective oxidation of styrene, the reaction was carried out in acetone as reaction medium with 25, 50, 100, 150 and 200 mg of catalyst for 18 h and 50 °C. The percentage conversion and percentage selectivity are shown in Fig. 9. The effect of amount of catalyst was studied keeping all other parameters (reaction time, temperature, mole ratio of substrate: H_2O_2) constant. It can be seen from Fig. 9 that % conversion of styrene is 6.5 with 6.3% yield for 25 mg of catalyst. For 50 mg of catalyst the styrene conversion increases to 12.7 mol% with 11.6% yield. For the same reaction when carried out by using 100 mg of catalyst the styrene conversion suddenly increases to 45.1 mol% with 88.5 mol% selectivity and 39.9% yield. Upon further increase in catalytic amount up to 150 mg and 200 mg, catalyst shows lower styrene conversion of 36.4 mol% and 27.7 mol% with 30.3% and 22.8% yield of benzaldehyde, respectively. At the lower catalyst loadings, the increase in the styrene conversion with the catalyst loading is due to the availability of more surface area, which enhances the styrene oxidation rate. However, at the higher catalyst loadings, the H_2O_2 decomposition rate is much higher than that at lower loading due to which sufficient H_2O_2 is not available for the oxidation, which ultimately leads to a lower styrene conversion. Also, at higher amount of catalyst adsorption or chemisorptions of two reactants on separate catalyst particles may be done, thereby reducing the chance to interact with each other, resulting in lowering the activity. Thus the catalyst loading (0.1 g) has an optimum value for obtaining the highest styrene conversion in the oxidation.
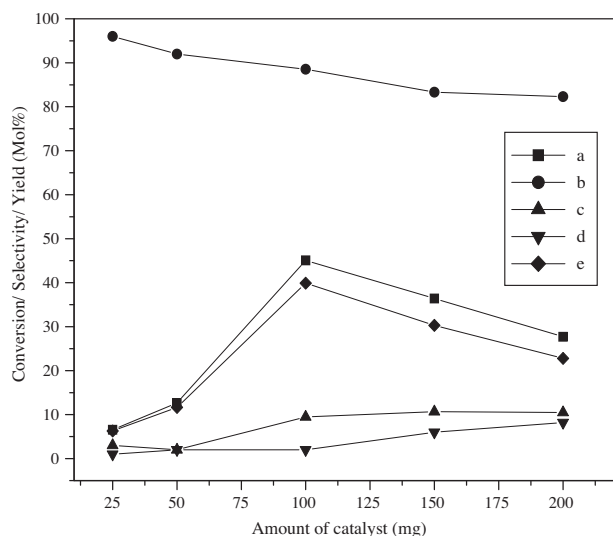

Figure 7 Effect of reaction temperature on styrene conversion and product selectivity over BaFe$_2$O$_4$ catalyst, (a) styrene conversion, (b) selectivity of benzaldehyde, (c) phenyl acetaldehyde, (d) others and (e) yield of benzaldehyde.

Figure 9 Effect of amount of catalyst on styrene conversion and product selectivity over BaFe$_2$O$_4$ catalyst, (a) styrene conversion, (b) selectivity of benzaldehyde, (c) phenyl acetaldehyde, (d) others and (e) yield of benzaldehyde.

4.6. Effect of oxidizing agents

The effect of different oxidants on the catalytic activity of BaFe$_2$O$_4$ toward styrene conversion and product distribution is also studied. Different oxidants such as H$_2$O$_2$, Urea-H$_2$O$_2$ (UHP) and *tert*-BuOOH were used as the oxygen source in acetone as solvent. The results are shown in Fig. 10. In the presence of 30% H$_2$O$_2$ the reaction proceeds with 45.1 mol% styrene conversion and 88.5 mol% selectivity of benzaldehyde, while the yield of benzaldehyde under this condition is 39.9%. When the same reaction was carried out in the presence of *tert*-BuOOH as oxidizing agent the styrene conversion takes place up to 38.6 mol%, but the selectivity of benzaldehyde decreased to 81.6 mol% with 31.5% yield. In the presence of ureated hydrogen peroxide (UHP), the styrene conversion reduced to 26.4 mol% with 74.2 mol% selectivity and 19.6% yield of benzaldehyde, respectively. In terms of percentage yield of benzaldehyde, the oxidizing agents show the efficiency in the order of H$_2$O$_2$ (30%) > *tert*-BuOOH > UHP. Among these oxidants H$_2$O$_2$ (30%) shows the better performance since it can give good oxidation conversion; moreover it generates only water as by-product; and it has high content of active oxygen.

4.7. Effect of sonication time

To examine the influence of ultrasonic treatment on the activity of barium ferrite, it was sonicated for different times in the reaction solvent and then the styrene and H$_2$O$_2$ were added successively in the reaction vessel. The results are shown in Fig. 11. When the catalyst is used without sonication the styrene conversion is 25.1 mol% with 90 mol% selectivity and 22.8% yield of benzaldehyde. The same catalyst when used by ultrasonic treatment for 5, 10 and 15 min the styrene conversion gradually increases from 29.4 mol% to 45 mol% along with increase in % yield from 26.3% to 39.9%, respectively. When the same reaction was carried out over the catalyst
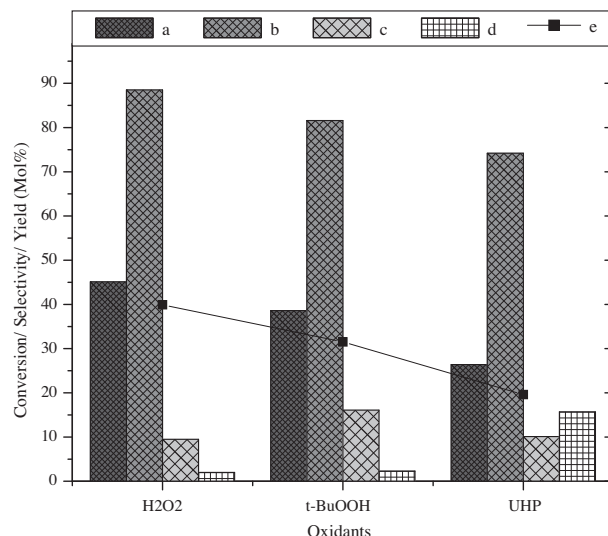

Figure 10 Effect of oxidizing agent on styrene conversion and product selectivity over BaFe$_2$O$_4$ catalyst, (a) styrene conversion, (b) selectivity of benzaldehyde, (c) phenyl acetaldehyde, (d) others and (e) yield of benzaldehyde.

which is sonicated for 20 min, the styrene conversion increases marginal to 45.6 mol% with reduction in the selectivity of benzaldehyde to 83.5 mol% and 38% yield. Sonication mostly affects reaction rate, yield and in some cases even the ratio of reaction products. This is due to the exposure of active sites on the surface of catalyst which may enhance the adsorption of styrene and H$_2$O$_2$, bring mechanical effects and induce cavities, which promotes the reactions. Secondly, the reaction proceeds in the presence of acetone and aqueous H$_2$O$_2$ which is hydrophobic in nature. In hydrophobic reactions normally the reagents get hidden inside the clusters due to which they are unavailable for the reaction. On ultrasonic treatment, ultrasound breaks these hydrophobic clusters, which make the reagent again available and thus acceleration of the reaction is observed.
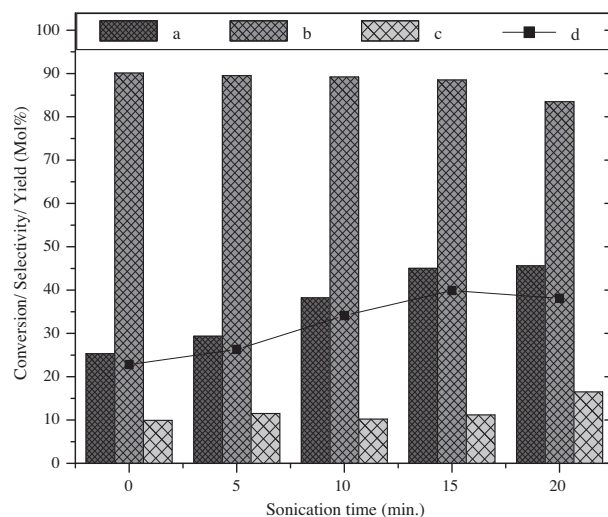

Figure 11 Effect of sonication time on styrene conversion and product selectivity over BaFe$_2$O$_4$ catalyst, (a) styrene conversion, (b) selectivity of benzaldehyde, (c) phenyl acetaldehyde and (d) yield of benzaldehyde.

5. Comparison of catalytic activity of AEM ferrites toward the selective oxidation of styrene

The selective oxidation of styrene to benzaldehyde is carried over the surface of a number of transition metal ferrites such as $NiFe_2O_4$ and $ZnFe_2O_4$. (Guin et al., 2005; Ramanathan and Sugunan, 2007) along with the alkaline earth metal ferrites like $MgFe_2O_4$ (Ma et al., 2003), $CaFe_2O_4$ (Pardeshi and Pawar, 2010), $SrFe_2O_4$ (Pardeshi and Pawar, 2011) and $BaFe_2O_4$. In comparison with transition metal ferrites, (AEM) ferrites show better catalytic activity because as it is known in most of the cases the catalytic activity of the catalyst depends on the chemical composition or cation distribution between the tetrahedral and octahedral site. Also, it may be due to the relative size of ion compared to the size of the lattice site and the site preference energy value of individual cation toward the A and B sites of the catalyst (Baldha et al., 2002). In case of divalent metal ions most of them are having smaller atomic size than the ionic size of Fe^{3+} ions. In transition metal ferrites, Fe^{2+} and Fe^{3+} are present in octahedral and tetrahedral coordination, while in alkaline earth metal ferrites; Fe^{3+} is present only in tetrahedral coordination (Candeia et al., 2007). Among various alkaline earth metal ferrites, $BaFe_2O_4$ is found to be a better catalyst even though they are prepared by same method (citrate gel combustion method). In case of $BaFe_2O_4$ (present work) 45.1 mol% of styrene conversion is observed with 88.5 mol% selectivity and 39.9% yield of benzaldehyde. While in case of $MgFe_2O_4$ (Ma et al., 2003) only 13.5 mol% styrene gets converted with 47.1 mol% selectivity and 6.46% yield of benzaldehyde. When the same reaction was carried under the similar experimental conditions over the surface of $CaFe_2O_4$ (Pardeshi and Pawar, 2010) the styrene conversion and % yield of benzaldehyde are 37.9 mol% and 91.1 respectively, while in case of $SrFe_2O_4$ (Pardeshi and Pawar, 2011) the styrene conversion and % yield of benzaldehyde are 63.7 mol% and 32.4, respectively. Along with the cation distribution the catalytic activity depends on the size of the ions. In case of barium ferrite the ionic size is 1.35 Å which is greater than the ionic size of Mg (0.78 Å), Ca (0.85 Å) and Sr (1.13 Å). The divalent metal ions are generally larger in size than trivalent metal ions. The octahedral sites are also larger than tetrahedral sites, in other ferrites, Fe^{2+} and Fe^{3+} are present in octahedral and tetrahedral coordination, while, in case of barium ferrite ionic size of Ba is 1.35 Å which is comparatively greater than iron (0.67 Å) which is present only in the tetrahedral coordination. Due to this variation in ionic size the $BaFe_2O_4$ may be showing the best catalytic activity among all the AEM ferrites.

6. Reusability of catalyst

The reusability of the $BaFe_2O_4$ is checked by using the utilized catalyst in the next cycles. Catalyst deactivation may occur due to chemical, mechanical and thermal reasons (Sato et al., 1996). The chemical deactivation is common in catalyst and caused by strong chemisorptions of species which blocks the active sites of the catalyst. In the first cycle at optimized conditions the styrene conversion and selectivity of benzaldehyde are up to 45.1 mol% and 88.5 mol%, respectively. $BaFe_2O_4$ was used after simple filtration for separation and washing with water and acetone and drying at 150 °C. The catalyst

was used at least for three cycles by 13.5% loss in activity, the results are shown in Fig. 12; furthermore the XRD pattern (not shown) of the reused catalyst was identical to that of the original, indicating that the crystallinity of the catalyst was not affected during the reaction.

7. Conclusions

$BaFe_2O_4$ spinel type catalyst is synthesized by the citrate-gel combustion method, the only method to synthesize soft ferrite other than the Pechini method. Thermal analysis of barium iron citrate precursor gives the information about the temperature (900 °C) at which the formation of barium ferrite takes place. The elemental analysis by XRF and metal oxygen stretching frequencies are confirmed by FTIR. The morphology by SEM suggests that the catalyst shows coralloid morphology with outward extending branches. XRD analysis confirmed the formation of single phase $BaFe_2O_4$ with trace quantity of adsorbed CO_2.

The catalytic activity studies show that $BaFe_2O_4$ is an efficient catalyst for selective oxidation of styrene in acetone as a solvent, in the presence of 30% H_2O_2 as oxidizing agent, which exhibits high activity and high selectivity. The styrene oxidation catalyzed by $BaFe_2O_4$ without using any phase transfer catalyst leads to the conversion of styrene up to 45.1 mol% along with the selectivity of benzaldehyde (88.5 mol%) with 39.9% yield as major product, while obtaining styrene oxide (9.5 mol%) as minor product, which quickly isomerizes into phenyl acetaldehyde.

Temperature 50 °C, time 18 h, styrene/H_2O_2 molar ratio as 1, aprotic and polar solvent like acetone, and catalyst amount 0.1 g, favor the selective oxidation of styrene.

Solvents have marked influence on the product distribution in selective oxidation of styrene; acetone seems to be the best solvent. The selectivity of benzaldehyde with respect to percentage yield for various solvents is in the order $CH_3COCH_3 > CH_3CN > C_2H_5OH > CH_3OH > H_2O$.
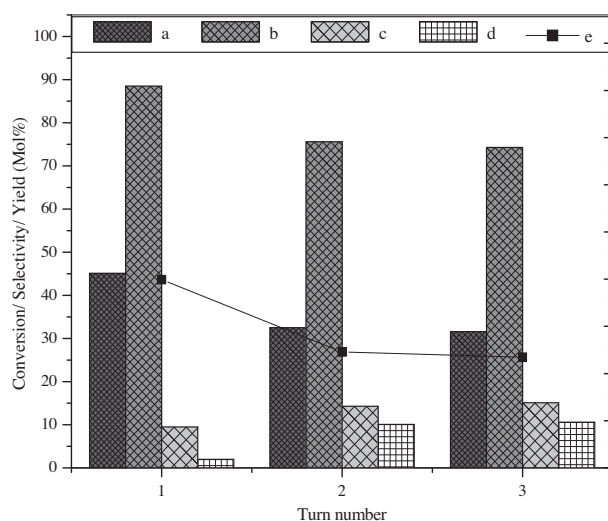

Figure 12 Effect of reusability on styrene conversion and product selectivity over $BaFe_2O_4$ catalyst, (a) styrene conversion, (b) selectivity of benzaldehyde, (c) phenyl acetaldehyde, (d) others and (e) yield of benzaldehyde.

The strong interaction between catalyst and H_2O_2 inhibits the coordination of substrate and enhances desorption of the products from the active sites, which prevents the deep oxidation of benzaldehyde to benzoic acid. The ultrasonication of reaction mixture exposes the active sites on the surface of catalyst, which enhances the adsorption of styrene, H_2O_2 and promotes the reaction. It also breaks the hydrophobic cluster and makes the reagents available to accelerate the reaction.

$BaFe_2O_4$ is found to be a better catalyst among all alkaline earth metal ferrites like $MgFe_2O_4$ $CaFe_2O_4$ and $SrFe_2O_4$ it may be due to different site preference energies of individual ions which depend on the ionic size of barium (1.35 Å) and iron (0.67 Å). Due to this almost all the Ba^{2+} ions occupy the octahedral lattice and equal number of Fe^{3+} ions occupies the tetrahedral lattice.

The catalyst could be used at least for three cycles with marginal (13.5%) loss in activity. The XRD pattern of the reused catalyst was identical to that of the original indicating that the crystallinity of the catalyst was not affected during the reaction.

Acknowledgement

References

Baldha, G.J., Saija, K.G., Modi, K.B., Joshi, H.H., Kulkarni, R.G., 2002. Study of cation distribution and macro-magnetic properties of magnesium and aluminum co-substituted lithium ferrite. Mater. Lett. 53, 233–237.

Bronoel, G., Grenier, J.C., Reby, 1980. Comparative behavior of various oxides in the various electrochemical reactions of oxygen evolution and reduction in alkaline medium. J. Electrochim. Acta 25, 1015–1018.

Busca, G., Daturi, M., Finocchio, E., Lorenzelli, V., Ramis, G., Willey, R.J., 1997. Transition metal mixed oxides as combustion catalysts: preparation, characterization and activity mechanisms. Catal. Today 33, 239–241.

Cabuil, V., 2000. Phase behavior of magnetic nanoparticles dispersions in bulk and confined geometries. Curr. Opin. Colloid Interface Sci. 5, 44–48.

Candeia, R.A., Souza, M.A.F., Bernardi, M.I.B., Maestrelli, S.C., Santos, I.M.G., Souza, A.G., Longo, E., 2007. Monoferrite $BaFe_2O_4$ applied as ceramic pigments. Ceram. Int. 33, 521–525.

Chin, T.S., Hsu, S.L., Deng, M.C., 1993. Barium ferrite particulate prepared by a salt melt method. J. Magn. Magn. Mater. 120, 64–68.

Clinard Jr, F.W., Hurley, G.F., Hobbs, L.W., Rohr, D.L., Youngman, R.A., 1984. Structural performance of ceramics in a high fluence fusion environment. J. Nucl. Mater. 123, 1386–1392.

Grenier, J.C., Pouchard, M., Hagenmuller, P., 1981. Vacancy ordering in oxygen deficient perovskite related ferrite. Struct. Bond. 47, 1–25.

Guin, D., Baruwati, B., Manorama, S.V., 2005. A simple chemical synthesis of nanocrystalline AFe_2O_4 (A = Fe, Ni, Zn): an efficient catalyst for selective oxidation of styrene. J. Mol. Catal. A: Chem. 242, 26–31.

Horvath, M.P., 2000. Microwave applications of soft ferrites. J. Magn. Magn. Mater. 215, 171–183.

Kumar, S.B., Mirajkar, S.P., Pais, G.C.G., Kumar, P., Kumar, R., 1995. Epoxidation of styrene over a titanium silicate molecular sieve TS-1 using dilute H_2O_2 as oxidizing agent. J. Catal. 156, 163–166.

Liu, X., Wang, J., Gan, L.M., Ng, S.C., Ding, J., 1998. An ultrafine barium ferrite powder of high coercivity from water in oil microemulsion. J. Magn. Magn. Mater. 184, 344–354.

Liu, X., Wang, J., Gan, L.M., Ng, S.C., 1999. Improving the magnetic properties of hydrothermally prepared barium ferrite. J. Magn. Magn. Mater. 195, 452–459.

Ma, N., Yue, Y., Hua, W., Gao, Z., 2003. Selective oxidation of styrene over nanosized spinel-type $Mg_xFe_{3-x}O_4$ complex oxide catalyst. Appl. Catal. A: Gen. 251, 39–47.

Meng, Y.Y., He, M.H., Zeng, Q., Jiao, D.L., Shukla, S., Ramnujan, R.V., Liu, Z.W., 2014. Synthesis of barium ferrite ultrafine powders by a sol-gel combustion method using glycine gels. J. Alloys Compd. 583, 220–225.

Nitani, N., Kuramoto, T., Yamashita, T., Nihei, Y., Kimura, Y., 2003. In-pile irradiation of rock-like oxide fuels. J. Nucl. Mater. 319, 102–107.

Pardeshi, S.K., Pawar, R.Y., 2010. Optimization of reaction conditions in selective oxidation of styrene over fine crystallite spinel-type $CaFe_2O_4$ complex oxide catalyst. J. Mater. Res. Bull. 45, 609–615.

Pardeshi, S.K., Pawar, R.Y., 2011. $SrFe_2O_4$ complex oxide an effective and environmentally benign catalyst for selective oxidation of styrene. J. Mol. Catal. A: Chem. 334, 35–43.

Ramanathan, R., Sugunan, S., 2007. Styrene oxidation by H_2O_2 using Ni-Gd ferrites prepared by co-precipitation method. Catal. Commun. 8 (10), 1521–1526.

Rezlescu, L., Rezlescu, E., Popar, P.D., Rezlescu, N., 1993. Fine barium hexaferrite powder prepared by the crystallisation of glass. J. Magn. Magn. Mater. 193, 288–290.

Sankaranarayanan, V.K., Pankhurst, Q.A., Dickson, D.P.E., 1993. An investigation of particle size effects in ultrafine barium ferrite. J. Magn. Magn. Mater. 125, 199–208.

Sato, K., Aoki, M., Ogawa, M., Hashimoto, T., Noyori, R., 1996. A practical method for epoxidation of terminal olefins with 30% hydrogen peroxide under halide-free conditions. J. Org. Chem. 61, 8310–8311.

Sato, K., Aoki, M., Ogawa, M., Hashimoto, T., Panyella, D., Noyon, R., 1997. A halide – free method for olefin epoxidation with 30% hydrogen peroxide. Bull. Chem. Soc. Jpn. 70, 905–915.

Sawada, H., 1996. Electron density study of spinel: magnesium titanium oxide (Mg_2TiO_4). Mater. Res. Bull. 31, 355–360.

Simmons, R.G., 1989. The effect of media properties on the longitudinal recording performance of particulate barium ferrite media. IEEE Trans. Magn. 25, 4051–4053.

Smith, J.R.L., Iamamoto, Y., Vinhado, F.S., 2006. Oxidation of alkanes by iodosylbenzene (PhIO) catalysed by supported Mn(III) porphyrins: Activity and mechanism. J. Mol. Catal. A: Chem. 252, 23–30.

Sugimoto, M., 1999. The past, present and future of ferrites. J. Am. Ceram. Soc. 82, 269–280.

Surig, C., Hampel, K.A., Bonnenberg, D., 1993. Formation and microwave absorption of barium and strontium ferrite prepared by sol-gel techniques. Appl. Phys. Lett. 63, 2836–2838.

Tang, X., Yang, Y.G., 2009. Composition and magnetic properties of M-Ba ferrite powders fabricated via sugar-nitrates process. Mater. Sci.-Pol. 27 (2), 529–537.

Viswanathan, B., Murthy, V.R.K., 1990. Ferrite Materials. Springer Verlag, Berlin.

Xu, P., Han, X., Jiang, J., Wang, X., Li, X., Wen, A., 2007. Synthesis and characterization of novel coralloid Polyaniline/$BaFe_{12}O_{19}$ nanocomposites. J. Phys. Chem. C 111, 12603–12608.